# STABILIZED FINITE ELEMENTS IN GEOMECHANICAL APPLICATIONS

S. Commend
*GeoMod consulting engineers, Lausanne, Switzerland*

Th. Zimmermann
*Zace services Ltd, Lausanne, Switzerland*

A. Truty
*Department of Environmental Engineering, Cracow University of Technology, Poland*

**ABSTRACT:** *In the framework of elastoplasticity, the use of low order finite elements is often desirable in order to simplify implementation, and also mesh generation. Unfortunately, standard low order elements behave poorly in incompressible and dilatant elastoplastic media, exhibiting pathologies such as volumetric locking and oscillations in the pressure field. In Commend (2001) & Commend et al. (2004), we proposed a novel approach to overcome such pathologies with the help of stabilized finite elements, earlier developed in the context of computational fluid dynamics. We recall here the key features of the approach, and present illustrations of the effectiveness for simple geomechanical applications in Z_Soil.PC (2009). In particular, the stabilized finite elements are shown to allow simultaneous use of low order quadrilaterals and triangles within the same mesh. Related work in two-phase media by the authors (see Truty and Zimmermann (2006)) is also briefly addressed.*

## 1 INTRODUCTION

The use of low order finite elements is often desirable in order to simplify mesh generation and also from an implementational point of view. Unfortunately such elements behave poorly in incompressible and dilatant elastoplastic situations, exhibiting pathologies such as volumetric locking and oscillations of the pressure field. Different techniques have been proposed in the literature to overcome this problem; in this paper we demonstrate the effectiveness of stabilization techniques, initially developed in the context of computational fluid dynamics and extended to a mixed displacement-pressure formulation of elastoplasticity in Commend (2001), on typical geomechanical applications. In section 2 we recall the governing equations, in section 3 we present the stabilization techniques, validation tests are presented in section 4, conclusions are finally drawn in section 5.

## 2 GOVERNING EQUATIONS

Eq. (1) defines equilibrium for the static case:

$$\mathrm{div}(\boldsymbol{\sigma}) + \mathbf{f} = 0 \tag{1}$$

where $\boldsymbol{\sigma}$ is the stress tensor and $\mathbf{f}$ the body load.

The incremental constitutive relation reads:

$$\boldsymbol{\Delta\sigma} = \mathbf{D}\left[\boldsymbol{\Delta\varepsilon} - \boldsymbol{\Delta\varepsilon}^{p}\right] \tag{2}$$

with $\mathbf{D}$ the elastic modulus matrix, $\boldsymbol{\Delta\varepsilon}$ the total strain increment and $\boldsymbol{\Delta\varepsilon}^{p}$ the plastic strain increment. The solution procedure is based on a discretized weak form in terms of displacement increments $\boldsymbol{\Delta\mathbf{u}}$. A mixed displacement-pressure form is obtained by introducing the following volumetric-deviatoric split into the constitutive equation for the stress increment:

$$\boldsymbol{\Delta\sigma} = \bar{\mathbf{D}}\left[\boldsymbol{\Delta\varepsilon} - \boldsymbol{\Delta\varepsilon}^{p}\right] + \mathbf{1}\Delta p \tag{3}$$

$\Delta p$, the hydrostatic pressure increment in the solid phase, can be expressed as:

$$\Delta p = K\Delta\varepsilon_{v}^{e} = K\mathbf{1}^{T}\left[\boldsymbol{\Delta\varepsilon} - \boldsymbol{\Delta\varepsilon}^{p}\right] \tag{4}$$

where $\Delta\varepsilon_{v}^{e}$ is the increment of the elastic volumetric strain and $K$ is the elastic bulk modulus. The deviatoric projection $\bar{\mathbf{D}}$ is defined as:

$$\bar{\mathbf{D}} = \mathbf{D}\left(\mathbf{I} - \frac{1}{3}\mathbf{1}\mathbf{1}^{T}\right) \tag{5}$$

where $\mathbf{I}$ is the identity matrix and $\mathbf{1}$ the vectorial representation of Kronecker's delta $\delta_{ij}$. A strong form of the problem can now be stated as follows: consider a body $\Omega$, its boundary $\partial\Omega = \Gamma = \overline{\Gamma_{g_i} \cup \Gamma_{h_i}}$ with $\Gamma_{g_i} \cap \Gamma_{h_i} = \varnothing$, with $i = 1,...,n_{sd}$, where $n_{sd}$ stands for the number of spatial dimensions. Given $f_i : \Omega \to \mathsf{R}$, $g_i : \Gamma_{g_i} \to \mathsf{R}$ and $h_i : \Gamma_{h_i} \to \mathsf{R}$, find $u_i : \bar{\Omega} \to \mathsf{R}$ and $p : \bar{\Omega} \to \mathsf{R}$ such that:

$$\sigma_{ij,j} + f_i = 0 \tag{6}$$

$$\varepsilon_{kk}^{e} - \frac{p}{K} = 0 \tag{7}$$

$$u_i = g_i \tag{8}$$

$$\sigma_{ij} n_j = h_i \tag{9}$$

where $\sigma_{ij}(\mathbf{u}, p)$ is computed incrementally using Eq. (3). A corresponding weak form is constructed by multiplying Eq. (6) and Eq. (7) by appropriate weighting functions, integrating by parts and making use of the natural boundary condition (see Commend et al. (2004)). Discretization then leads to a matrix form which we can solve for $\boldsymbol{\Delta\mathbf{u}}$ and $\boldsymbol{\Delta\mathbf{p}}$:

$$\begin{bmatrix} \mathbf{K}_{uu} & \mathbf{K}_{up} \\ \mathbf{K}_{pu} & \mathbf{K}_{pp} \end{bmatrix} \begin{Bmatrix} \boldsymbol{\Delta\mathbf{u}} \\ \boldsymbol{\Delta\mathbf{p}} \end{Bmatrix} = \begin{Bmatrix} \mathbf{F}_{u} \\ \mathbf{F}_{p} \end{Bmatrix} \tag{10}$$

where $\mathbf{F}_{u}$ and $\mathbf{F}_{p}$ are generalized out-of-balance forces at current load step and iteration.

The nonlinear problem is solved iteratively using Newton-Raphson method. Convergence of the described mixed approach is known to be dependent on the choice of interpolation functions adopted for displacement and pressure fields. Application of the same interpolation functions for both fields requires a certain stabilization term to be added to to the system expressed by Eq. (10) to avoid spurious oscillations in the pressure field in the incompressibility limit.

## 3 STABILIZATION TECHNIQUES

Following the approach applied by Hughes et al. (1986) for computational fluid dynamics - see also Franca (1987) and Hughes (1987) - we consider adding to the system of Eq. (10) stabilizing terms of the form:

$$\sum_{e=1}^{n_{el}} \int_{\Omega^e} \left( \mathbf{L}^T \boldsymbol{\sigma}\left(\mathbf{w}^h, q^h\right) \right)^T \boldsymbol{\tau} \left( \mathbf{L}^T \boldsymbol{\sigma}\left(\mathbf{u}^h, p^h\right) + \mathbf{f} \right) d\Omega \tag{11}$$

where $\boldsymbol{\tau} = \dfrac{\alpha^e (h^e)^2}{2\mu} \mathbf{I}$ (see Hughes et al. (1986)) is a stabilization factor matrix.

$h^e$ is the dimension of the element, $\mu$ the material's shear modulus and $\alpha^e$ a scalar parameter. $\mathbf{L}$ is a differential operator which has the effect of taking the divergence of $\boldsymbol{\sigma}$. The $^h$ superscript indicates discretized values, while $\mathbf{w}$ and $q$ are weighting functions. In the most general case, such a formulation affects both the upper and the lower part of the matrix system of Eq. (10). An heuristic search of the most appropriate weighting terms in Commend et al. (2004) leads, however, to a simpler formulation in which only the second equation in Eq. (10) is stabilized by the residual of the equilibrium equation weighted by a pressure term. This formulation is defined in the sequel as Galerkin plus pressure stabilization (GPS). The corresponding stabilization term is defined as (see Commend et al. (2004)):

$$\sum_{e=1}^{n_{el}} \int_{\Omega^e} (\nabla \mathbf{N})^T \boldsymbol{\tau} \left( \mathbf{L}^T \boldsymbol{\sigma}\left(\mathbf{u}^h, p^h\right) + \mathbf{f} \right) d\Omega \tag{12}$$

where $\mathbf{N}$ are pressure shape functions. This type of stabilization is used in all the subsequent analyses. Another possibility, first proposed in the field of computational soil mechanics by Pastor et al. (1997) is to consider stabilization terms of the form:

$$\sum_{e=1}^{n_{el}} \int_{\Omega^e} (\nabla \mathbf{N})^T \boldsymbol{\tau} (\nabla \mathbf{N}) d\Omega \tag{13}$$

This latter technique shows very similar results when compared to the GPS scheme in the benchmarks that we have analyzed. Finally, a directional character can be introduced in the stabilization terms, following the finite increment calculus formulation described by Oñate (2000) which yields:

$$\sum_{e=1}^{n_{el}} \int_{\Omega^e} (\nabla \mathbf{N})^T \frac{3}{8\mu} \mathbf{h}\mathbf{h}^T \left( \mathbf{L}^T \boldsymbol{\sigma}\left(\mathbf{u}^h, p^h\right) + \mathbf{f} \right) d\Omega \tag{14}$$

where **h** is a unitary directional vector depending on the last converged increment of displacement. Details on how this directional formulation provides a tentative physical justification to the GPS formulation can be found in Commend (2001).

## 4 VALIDATION TESTS

### *4.1 Bearing Capacity of a Superficial Footing*

This first example illustrates a classical geomechanical application. A superficial rigid foundation on an incompressible ($\psi$=0) medium is subjected to a increasing loading (Fig. 1), until failure is detected. Gravity loads are neglected ($\gamma$=0). Several analytical solutions to this problem exist in the literature (see Terzaghi (1951) or Matar and Salençon (1979)).

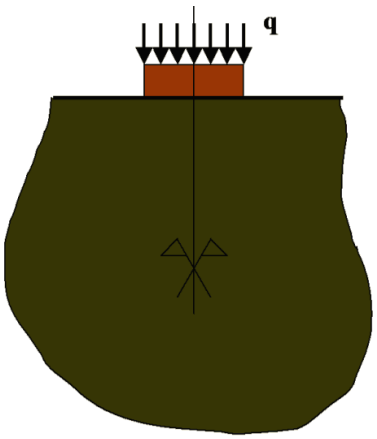


**E = 3000 kN/m² ; ν = 0.38 ; γ = 0**
**Drucker-Prager with size-adjustment on**
**Mohr-Coulomb (Z_SOIL.PC (2001))**
**c = 1 kN/m² ; ϕ = 20°**
**Dilatancy angle ψ = 0°**
**Surface load q = 0 → 20 kN/m**

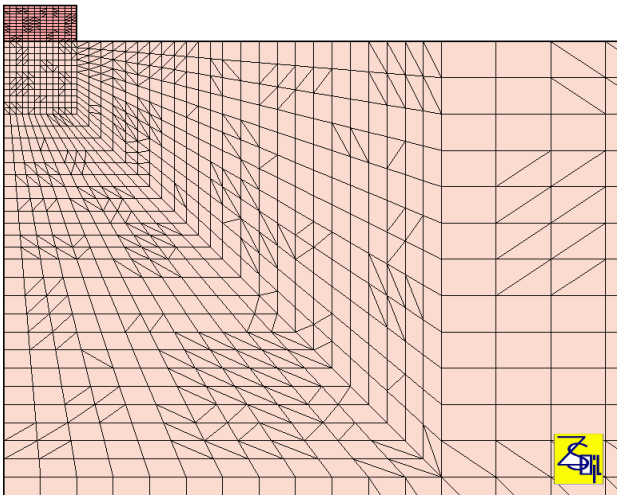

Fig. 1. Superficial footing geometry, and FE mesh composed of quadrilaterals (Q4) and triangles (T3)

Following Matar and Salençon (1979), the ultimate load for a rough footing is given by:

$$q_u = \mu_c \cdot c \cdot N_c^{'} \tag{15}$$

where $\mu_c$ and $N_c^{'}$ are scalar coefficients depending on the dimensions of the footing, friction angle $\phi$ and cohesion $c$. In our case, this theoretical solution gives $q_u = 1.05 \cdot 1 \cdot 14.83 = 15.6 \ \ KN/m$.

When standard bilinear displacement quadrilateral elements (Q4) are used to simulate incompressible media, results show an overshoot of theoretical solutions, characteristic of locking, this also holds for constant strain triangles, or when a mixture of the two types of elements is being used; similarly, dilatant media show the same locking phenomena.

Earlier solutions to overcome locking, like $\bar{\mathbf{B}}$ strain-projection (see Hughes (1987)), enhanced assumed strains (EAS) (in Simo and Rifai (1990)) or cross-diagonal triangles (in Nagtegaal et al. (1974)) solve the incompressible case for quads. EAS also overcomes locking for dilatant media when mesh is composed of quadrilaterals, but all fail when

quadrilaterals and triangles are used simultaneously within the same mesh, a situation which is often unavoidable.

In the present study, three different meshes are used: one composed of quads, another one composed of triangles and the third one containing a mixture of both types of elements (Figure 1). The proposed stabilized formulation slightly overshoots the limit load indicated by Q4B (BBAR) elements, which is equal 15.6 kN/m for the incompressible case (Figure 2). It yield results very close to the EAS one (16.3 kN/m). Mixture of T3/Q4 stabilized elements yields slightly stiffer response. The limit load in the dilatant case (Figure 4) indicated by EAS elements and stabilized as well is equal to 16.5 kN/m. The failure mechanism is reproduced in Figure 4 (dilatant case, $\psi$ = 10°) for the Q4 + T3 mesh. It is identified by displacement increments color maps between $q = 16.2\ \ kN/m$ and $16.4\ \ kN/m$.

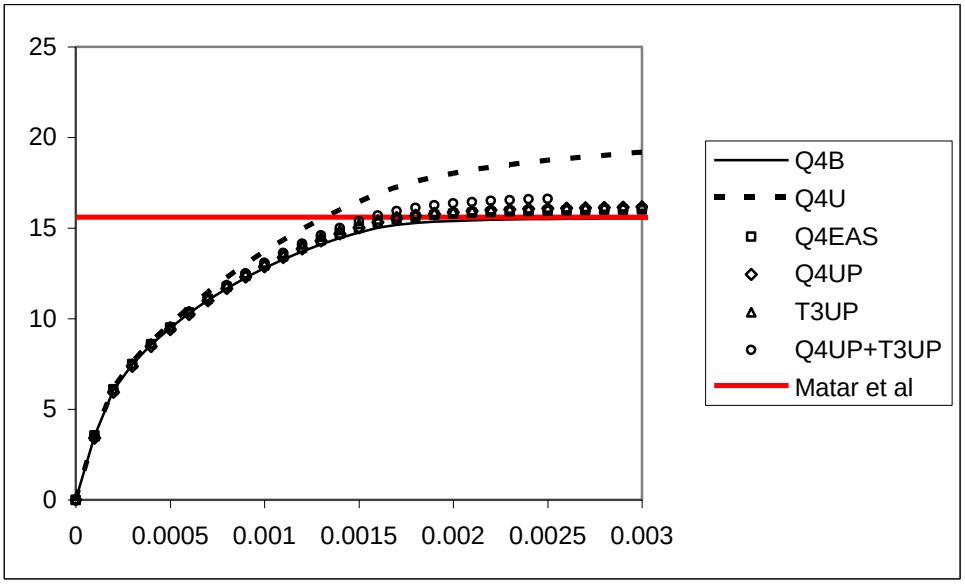


Fig. 2. Force-settlement diagram (incompressible case)

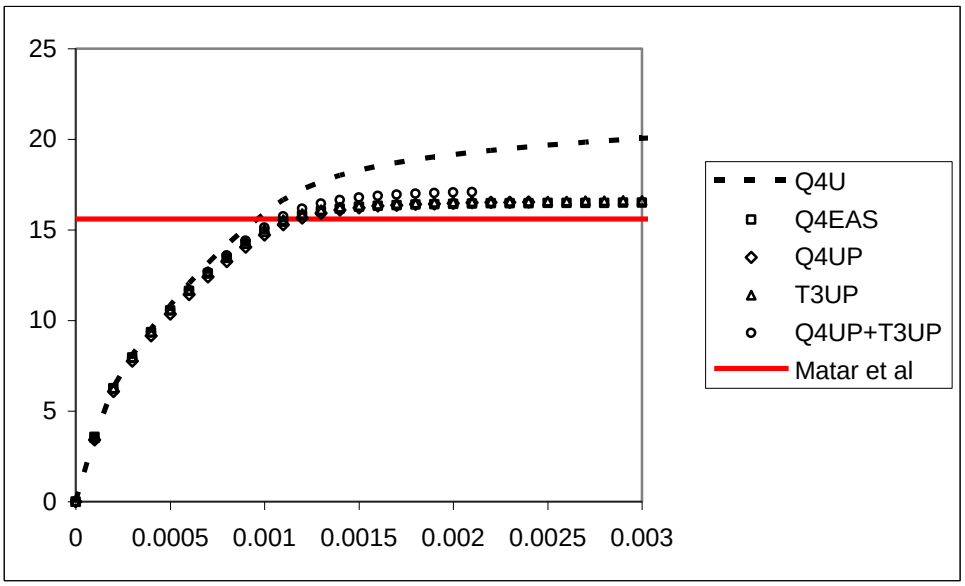


Fig. 3. Force-settlement diagram (dilatant case $\psi$ = 10°)

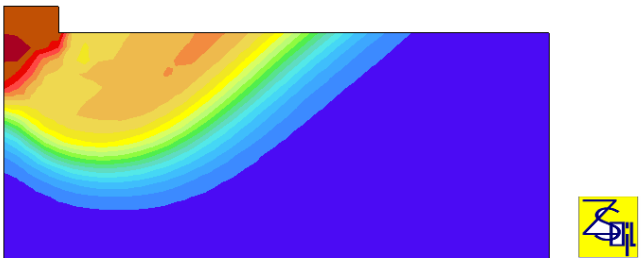

Fig. 4. Failure mechanism identified by displacement increments intensities (Q4+T3 mesh, dilatant case)

All tests have been performed with a stabilization parameter $\alpha^e = 1.0$, on a mesh of $15 \times 15$ meters with fixed boundary conditions at the bottom and sliding boundary conditions on both sides. The width of the footing is $2a = 2$ meters. The mesh is composed of 1296 quads, or 2592 triangles, or a mixture of both (only half of the footing has been modelled due to symmetry).

### *4.2 Rocking Foundation*

The case of a rocking foundation is considered next. A moment is applied to a superficial foundation of width $2a = 10$ meters under plane strain conditions, and we are looking for a limit moment and the associated failure mechanism. Geometry and properties of the soil are given in Figure 5.

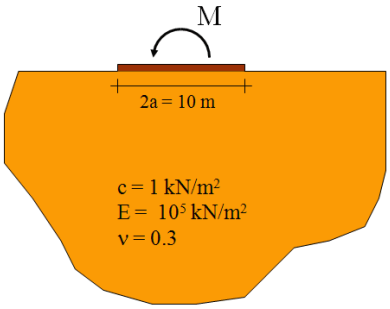


Fig. 5. Rocking foundation: geometry and properties

An estimate of the ultimate moment in the rigid-perfectly plastic case is defined in Yoder (1981):

$$\frac{M_u}{a^2 \tau_M} = (1 + \frac{\pi}{2}) \tag{16}$$

where $\tau_M$ is the shear strength of the medium, equal to cohesion $c$ if we use a Mohr-Coulomb model. Two types of meshes have been used in this study. First, a mesh composed of triangles and quads disposed in an elliptical pattern around the foundation. Second, a rectangular mesh pattern (6344 quads) of 80 meters depth and 100 meters width used to analyse the influence of mesh alignment with the failure mechanism. Results show that a failure mechanism can be found in both cases (see Figure 6). Results obtained with the stabilized approach are found to be between the theoretical limit moment and the results found by Yoder (1981), while standard Q4 elements overestimate the bearing capacity of the foundation (see Figure 7).

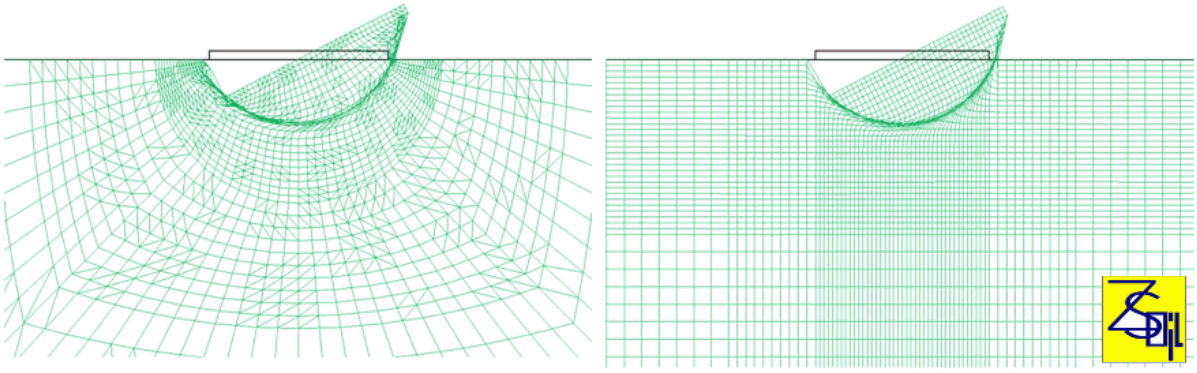

Fig. 6. Rocking foundation: failure mechanisms (left: elliptical Q4+T3 pattern, right: rectangular Q4 pattern)

| | $\frac{M_u}{a^2 \tau_M}$ |
|---|---|
| Yoder (theory) | 2.57 |
| Yoder (numerical) | 3.00 → 3.30 |
| **Q4 + T3 Stab** | **3.00** |
| **Q4 Stab (rect. pattern)** | **3.20** |
| Standard Q4 + T3 | > 8.00 |

Fig. 7. Recapitulation of results

The same rocking foundation test is reproduced next with boundary conditions closer to the foundation in an incompressible elastic medium in order to show the effect of stabilization on pressure oscillations. Figure 8 shows isolines of the first stress invariant $I_1(\boldsymbol{\sigma})$ for the mixed unstabilized case (left), and for the stabilized solution (right). Instabilities noticed in the former case are clearly overcome in the latter one.

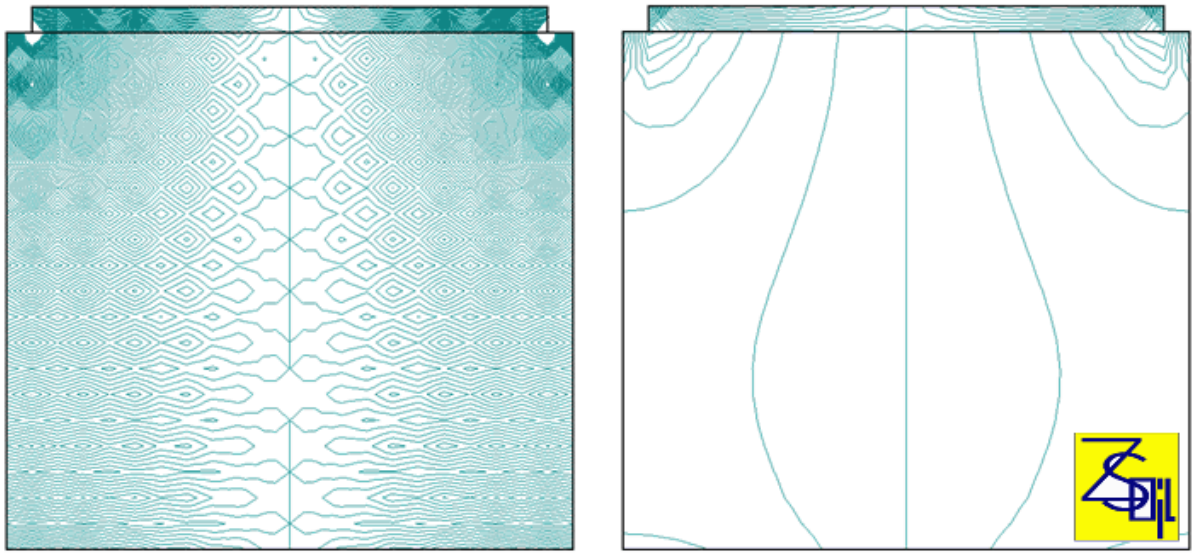

Fig. 8. First stress invariant isolines (left: standard mixed formulation, right: stabilized solution)

*4.3 Convergence Study on the Thick Cylinder Test*

In Commend et al. (2004) we present a convergence study on a nearly incompressible elasto-plastic thick cylinder loaded by an internal pressure (Figure 9).

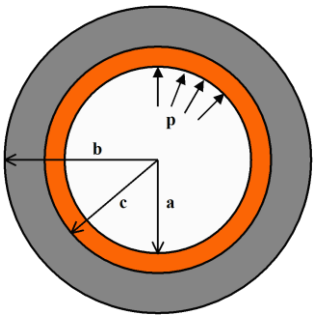


Fig. 9. Elasto-plastic thick cylinder loaded by an internal pressure

The existence of an analytical solution makes it possible to prove convergence when mesh size h is refined, on the normalized $L_2^*$ pressure and displacement error norms.

In particular, Figure 10 compares the evolution of the error with respect to $N$ - the number of elements in the radial direction of the cylinder - for two internal pressures, and for two different finite element meshes: $\overline{\mathbf{B}}$ enhanced Q4 elements vs. a mixture of GPS stabilized Q4+T3 elements.

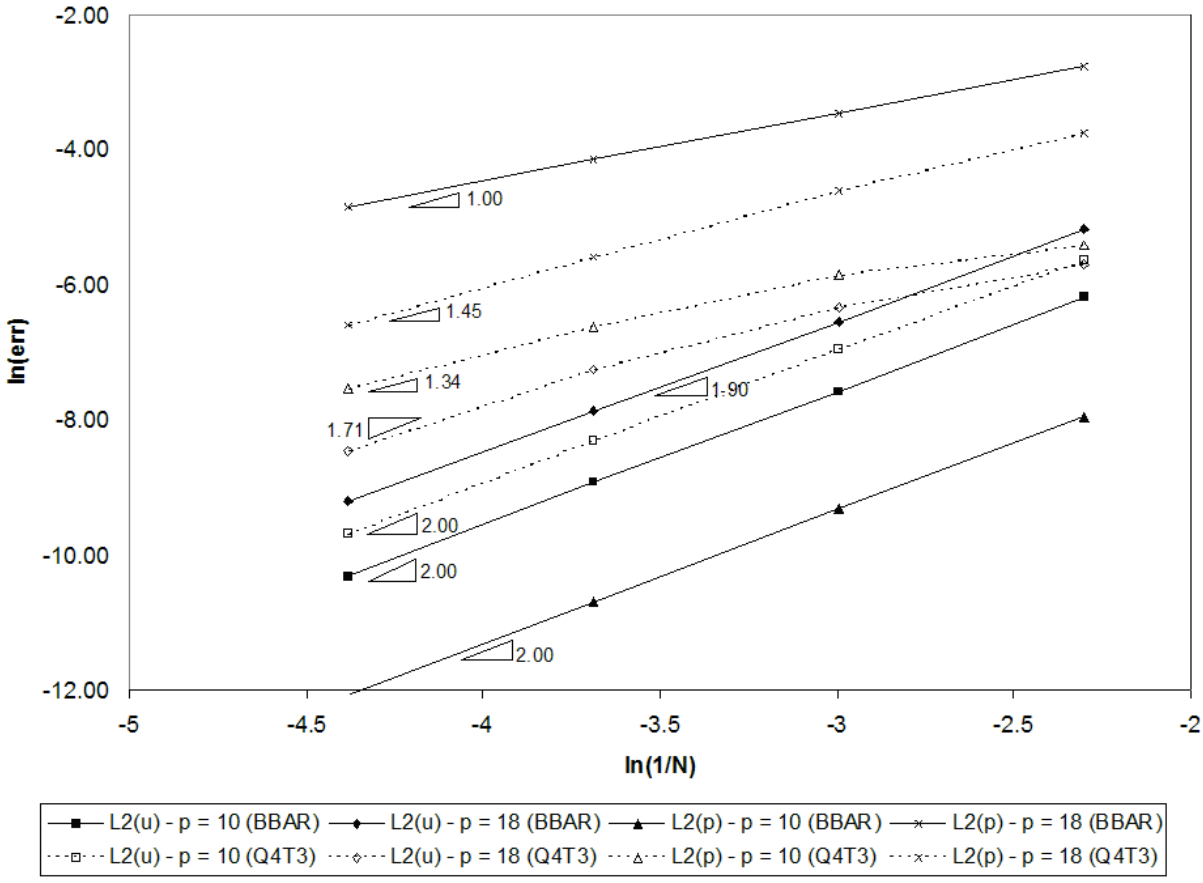


Fig. 10. Convergence study on the thick cylinder test

*4.4 Stabilization in two-phase media: Consolidation Analysis of a Superficial Footing*

It is also possible to apply such stabilization techniques to two-phase media consolidation problems in order to circumvent violation of the LBB condition, leading to spatial pressure oscillations when the same interpolation fields are used for both displacement and pore pressure fields. Different classes of stabilized methods are described in Truty and Zimmermann (2006). To illustrate the efficiency of the approach, Figure 11 shows the pore pressure distribution in a consolidation analysis of a superficial footing, and it is shown that while standard elements exhibit strong oscillations in the pressure field, stabilized elements overcome this problem and yield a smooth solution. The formulation adopted here combines the enhanced assumed strains (EAS) for the solid with stabilization for the fluid pressure equation.

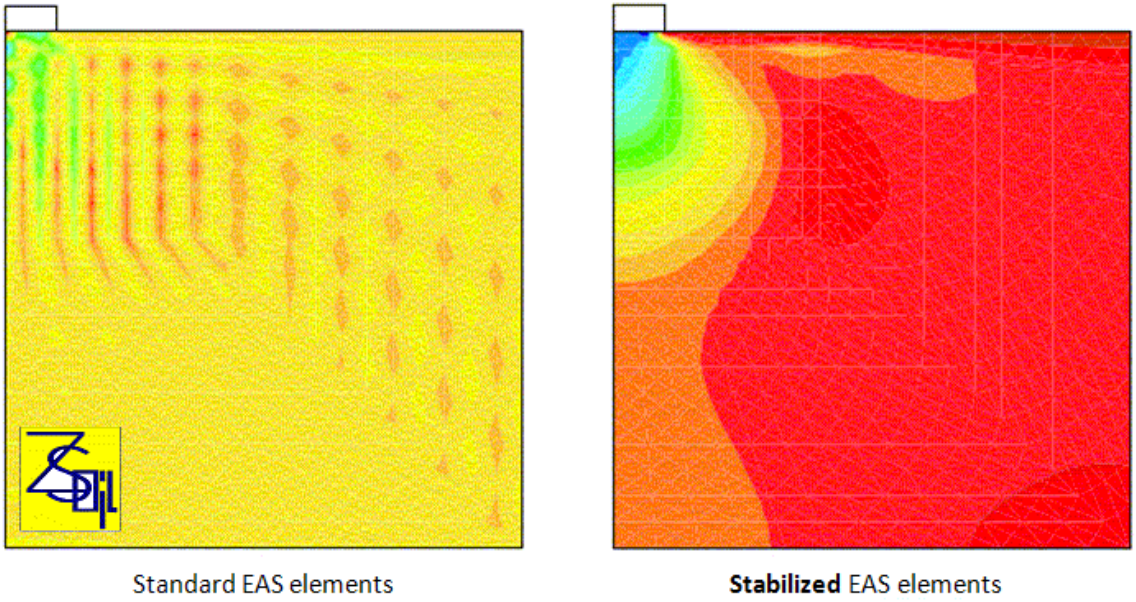


Fig. 11. Pore pressure contours at t = 0.1 years

## 5 CONCLUSIONS

The performance of stabilized finite element formulations is examined in this paper. A novel stabilization scheme developped in Commend (2001) and Commend et al. (2004) and applied here to a mixed displacement-pressure formulation of elastoplasticity is used. The proposed formulation is shown to provide an appropriate remedy to problems of locking in incompressible and dilatant media and allows the use of low order quadrilateral and triangular elements, including in association with a mixture of triangular and quadrilateral elements within the same mesh. Illustrations on classical geomechanical applications are presented, which demonstrate the effectiveness of the approach.

## ACKNOWLEDGEMENT

The financial support of the Fund of the Swiss National Committee on Large Dams and of the Swiss National Science Foundation under grant 21-49404.96 for the first author is gratefully acknowledged.

## REFERENCES


Commend, S. (2001), "Stabilized Finite Elements in Geomechanics", PhD Dissertation 2391, Swiss Federal Institute of Technology (EPFL), Lausanne

Commend, S., Truty, A. and Zimmermann, Th. (2004), "Stabilized Finite Elements Applied to Elastoplasticity: I. Mixed Displacement-Pressure Formulation", Comp. Meth. in Appl. Mech. and Eng., Vol. 193, 3559-3589

Franca, L.P. (1987), "New Mixed Finite Element Methods", PhD Dissertation, Stanford University, Palo Alto (CA)

Hughes, T.J.R., Franca, L.P. and Balestra, M. (1986), "A New Finite Element Formulation for Computational Fluid Dynamics: V. Circumventing the Babuska-Brezzi Condition: A Stable Petrov-Galerkin Formulation of the Stokes Problem Accomodating Equal-Order Interpolations", Comp. Meth. in Appl. Mech. and Eng., Vol. 59, 85-99

Hughes, T.J.R. (1987), The Finite Element Method: Linear Static and Dynamic Finite Element Analysis, Prentice-Hall.

Hughes, T.J.R., Franca, L.P. and Balestra, M. (1989), "A New Finite Element Formulation for Computational Fluid Dynamics: VIII. The Galerkin/Least-Squares Method for Advective-Diffusive Equations", Comp. Meth. in Appl. Mech. and Eng., Vol. 73, 173-189

Matar, M. and Salençon, J. (1979), "Capacité portante des semelles filantes", Revue Fr. de Géotechnique, Vol. 9, 51-76

Nagtegaal, J.C., Parks, D.M. and Rice, J.R. (1974), "On Numerically Accurate Finite Element Solutions in the Fully Plastic Range", Comp. Meth. in Appl. Mech. and Eng., Vol. 4, 153-177

Oñate, E. (2000), "A Stabilized Finite Element Method for Incompressible Viscous Flows Using a Finite Increment Calculus Formulation", Comp. Meth. in Appl. Mech. and Eng., Vol. 182, 355-370

Pastor, M., Quecedo, M. and Zienkiewicz, O.C. (1997), "A Mixed Displacement-Pressure Formulation for Numerical Analysis of Plastic Failure", Computers and Structures, Vol. 62(1), 13-23

Simo, J.C. and Rifai, M.S. (1990), "A Class of Mixed Assumed Strain Methods and the Method of Incompatible Modes", Int. J. Num. Meth. Eng., Vol. 29, 1595-1638

Terzaghi, K. (1951), Mécanique théorique des sols, Dunod, Paris

Truty, A. and Zimmermann, Th. (2006), "Stabilized mixed finite element formulations for materially nonlinear partially saturated two-phase media", Comp. Meth. in Appl. Mech. and Eng., Vol 195, 1517-1546

Yoder, P.J. (1981), "A Strain-Space Plasticity Theory and Numerical Implementation", PhD Dissertation, Californian Institute of Technology

Z_Soil.PC (2009), User manual, Zace services Ltd, Lausanne